Electronic states and surface structure of $PdTe_2$ as probed by scanning tunneling microscopy and photoemission spectroscopy

George W. Ryan and Wayne L. Sheils
School of Physics, LaTrobe University, Bundoora, Victoria 3084, Australia
(Received 28 December 1998; revised manuscript received 23 April 1999)

Images of the basal plane of palladium ditelluride ($PdTe_2$) taken with a scanning tunneling microscope are discussed with the aid of scanning tunneling spectroscopy (STS) and angle-resolved photoemission results taken from the same material. Two states associated with transitions into unoccupied bulk conduction bands are observed at 0.5 eV and 1.7 eV. The STS results compare well with theoretical calculations of the density of states of $PdTe_2$. In addition, the position of features in the STS spectra are found to compare closely with peaks appearing in the photoemission spectra taken at normal emission and peaks in the inverse photoemission spectra taken at normal incidence. As well as identifying the tellurium atoms as the main source of tunneling current for low bias voltages, the STS results provide experimental evidence that the scanning tunneling microscope preferentially samples states that exist along the ΓA symmetry line of the Brillouin zone in this material.

The chemical identity of the atomic positions seen in high-resolution scanning tunneling microscopy (STM) images cannot be determined from the topographical data. This shortcoming of STM becomes particularly evident for samples comprised of more than one element. Important additional information on the source of the tunneling current can be obtained by collecting current versus voltage spectra in conjunction with STM images. To be useful, however, the observed scanning tunneling spectra need to reveal resonances that can be compared with other spectroscopic results for the material in question. Access to photoemission and inverse photoemission spectra is very helpful in this regard because established band-structure theories often allow the observed peaks to be confidently assigned to specific electron states. When similar features appear at the same energy in scanning tunneling spectroscopy (STS) data, it may be possible to use the same band-structure knowledge to identify the source atoms.[1,2]

Atomic sites have been successfully identified on semiconductor surfaces with the aid of spatially resolved STS data collected during the topographical scan of the surface.[3,4] Spatially resolved STS data is preferable but not necessarily essential for this task. The most important requirement is a method that detects all the current versus voltage resonances with energy levels close to the bias voltages used to collect the atomic resolution images. Many metals and metal alloys produce stable and reproducible images for bias voltages within 500 mV of the Fermi level without having the dangling-bond or prominent surface states that would make it easy to identify the atoms being imaged.[5] For such samples assistance can be obtained by resorting to STS techniques that maximize the collection of well-averaged spectra capable of revealing weaker bulk states. We have used a spatially averaged form of STS specially designed to detect low amplitude electron states. In addition, we have collected angle-resolved inverse photoemission data and used previously published photoemission data to compare with the STS results.[6]

There has been considerable debate over the identity of the most prominent atomic sites appearing in the STM images taken from some transition-metal dichalcogenides. In some cases the brightest features in the STM images have been attributed to the underlying metal atoms.[7] This paper contributes to this debate by focusing on palladium ditelluride ($PdTe_2$), a metallic material belonging to group VIII of the transition metal dichalcogenides.[8] Both metal *d* bands and tellurium *p* bands contribute to the density of states (DOS) in the vicinity of the Fermi energy of this layered material[6,9] making it particularly difficult to say which species of atom is contributing most to the tunneling current.

Palladium ditelluride has the same structure as cadmium iodide with a hexagonal unit cell and Brillouin zone as shown in Fig. 1.[6,8,9] One layer of $PdTe_2$ consists of a hexagonally arranged plane of palladium atoms lying between two planes of hexagonally close-packed tellurium atoms. The prismatic symmetry of the compound means that alternate layers are arranged in an ABC pattern in the bulk crystal. Thus one Te-Pd-Te layer is sufficient to define the unit cell in the *c* direction. The bonding between the atoms in each layer is predominantly covalent. The bottom plane of tellurium atoms in one layer faces the upper plane of tellurium from the layer below. The bonds between adjoining layers of tellurium atoms are attributable to weak Van der Waals forces and are easily broken by cleaving. The ease with which the samples could be cleaved to produce clean flat crystalline surfaces leads to the inference, drawn by other authors studying other transition-metal dichalcogenides, that the surface terminates with a layer of chalcogenide atoms.[7,10]

Freshly cleaved samples of $PdTe_2$ were imaged in air and in UHV (base pressure $<1\times10^{-9}$ Torr). For the experiments carried out in UHV, the sample was cleaved in air using adhesive tape and immediately transferred to the UHV system, where it was heated to 200 °C for 2 h and then allowed to cool to ambient temperature. The hexagonal structure of $PdTe_2$ is clearly seen in the STM images in Fig. 2. Three rows of prominent high current (white) spots, each oriented

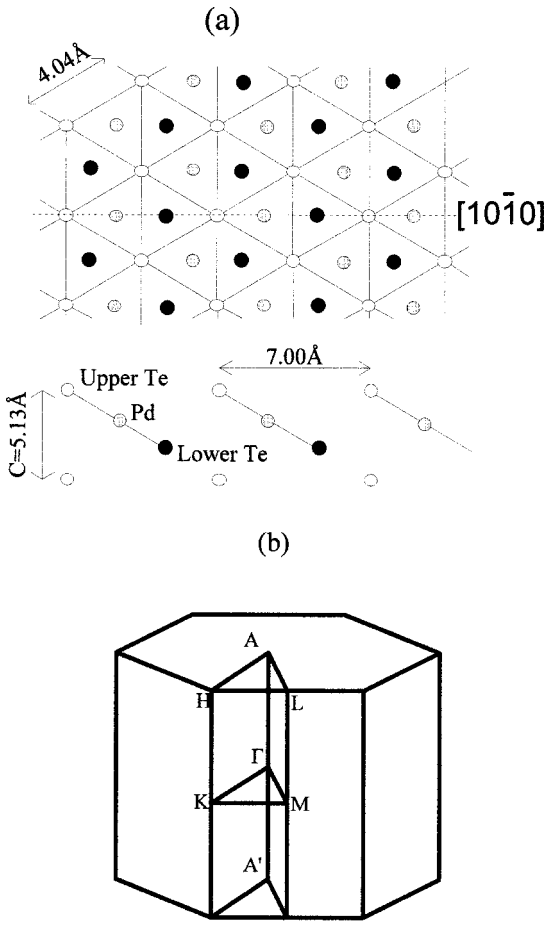

FIG. 1. (a) The (0001) surface structure of $PdTe_2$ and a cross section taken along the $[10\bar{1}0]$ direction (dashed line) to show the $(11\bar{2}0)$ plane. (b) The three-dimensional Brillouin zone for $PdTe_2$.

at 120° to the other, can be seen in the constant height images shown in Fig. 2. Figure 2(a) is an image taken in air with a set point current of 7.3 nA and a bias voltage of 4 mV, and Fig. 2(b) is a UHV image taken with the current set at 0.36 nA and the bias at -0.199 V. The choice of current and bias in Fig. 2(a) suggests this image was most likely taken with the tip closer to the surface than was the case in Fig. 2(b). The distance 4.0 ± 0.1 Å between the bright spots in the images in Fig. 2 matches the interatomic distance measured by x-ray diffraction,[11] indicating every atom in one layer of the crystal makes an equal contribution to the image. It is not however possible to decide whether the brightest spots emanate from a plane of tellurium atoms or from a plane of palladium atoms. In some parts of the images, it is possible to make out a second hexagon of atomic sites of intermediate intensity interposed between the bright and dark ones along the $[10\bar{1}0]$ direction [see Fig. 1(a)]. It is possible that such sites, which have been observed in other transition-metal dichalcogenides,[10] originate from a second layer in the crystal.

Spatially resolved STS requires the feedback controller to be disabled while the bias voltage is ramped.[3,12] The voltage excursion must be performed quickly to allow the bias to settle back to its starting dc level for the resumption of imaging before drift alters the position of the instrument. On metal surfaces where the tunneling current rises rapidly with

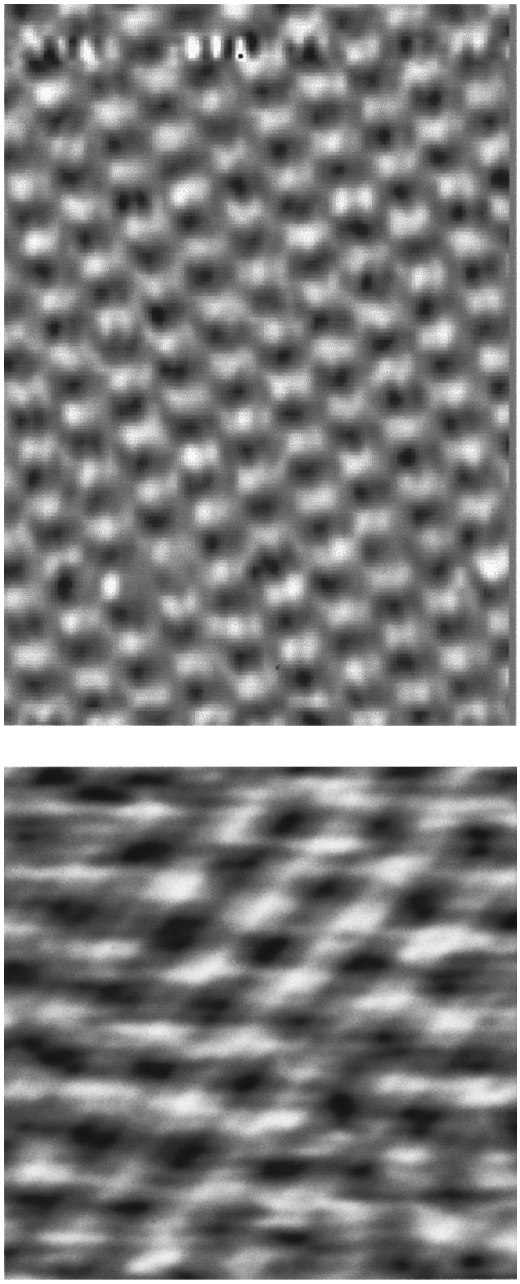

FIG. 2. Constant-height STM images of the basal plane of $PdTe_2$. The bright areas corresponding to regions of higher tunneling current are considered to refer to the sites of the uppermost layer of tellurium atoms. (a) 33×49 Å^2 image obtained in air with a tip voltage 4 mV and a set point current 7.3 nA. (b) 25×25 Å^2 image acquired in UHV with a tip voltage -199 mV and a set point current 0.36 nA.

applied voltage, the technique can become unstable. Furthermore, the sharp tips required for atomic resolution do not generally produce the best STS data.[2,13] Current versus voltage data can be obtained without disrupting the electronic control circuit by adding an ac component to the dc bias voltage at a frequency well beyond the circuit's cutoff frequency.[14] A 2 V oscillation can be used to investigate states within 2 eV of the Fermi level (E_F) of a sample with the energy resolution obtained dependent on how much current data can be collected each cycle. The number of voltage

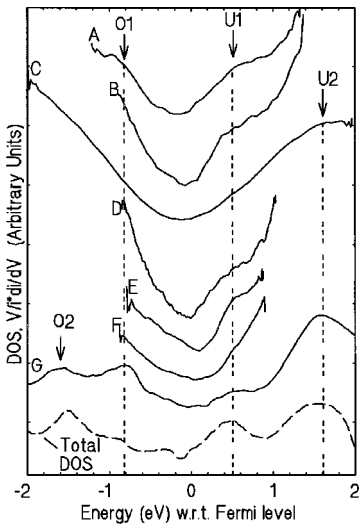

FIG. 3. Normalized differential conductance ($V/I^*dI/dV$) spectra taken from $PdTe_2$ samples. Curves $A-C$ were acquired in UHV, curves $D-G$ in air. A tungsten tip was used for curve D and PtIr tips for the other experiments. Curves D and G average 90 cycles of a 296 Hz voltage oscillation, while the remaining curves come from 200 cycles of a 1 kHz oscillation. The dc voltages varied between 0.55 V and 0.28 V and the set point currents between 0.03 nA and 0.37 nA. The bottom dashed curve is the calculated total DOS for $PdTe_2$ taken from Ref. 9.

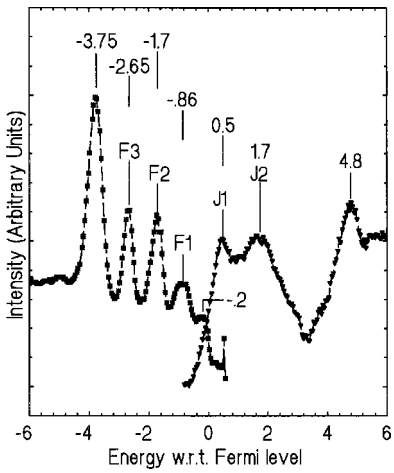

FIG. 4. Normal-emission photoelectron spectrum (left) and normal-incidence inverse photoemission spectrum (right) of $PdTe_2$. The features with the indicated energy levels are discussed in the text. Photons with an energy of 16.8 eV were used to acquire the spectrum on the left while the right-hand spectrum was recorded at a photon energy of 11.4 eV. Both spectra have been smoothed and corrected for the effects of the respective detectors (see Refs. 15 and 16).

cycles that can be collected and averaged depends only on the capacity of the data acquisition system and not on the stability of the tunneling junction.

In the STS experiments, which led to the spectra shown in Fig. 3, the oscillating bias signals were derived from computer-generated square waves that could be synchronized with the 100 kHz square wave used to trigger the collection of each current reading. Ninety or more cycles of data were averaged and any capacitive current removed to provide a single averaged I-V curve.[14] The averaged I-V curves were then numerically differentiated and divided by I/V to flatten and normalize the spectra.[13] Curves $A-C$ in Fig. 3 are normalized STS spectra of $PdTe_2$ taken from an STM operating in UHV. Curves $D-G$ were taken with an STM operating in air. All curves are plotted with respect to the Fermi level, i.e., with respect to the negative tip bias voltage. The dashed curve at the bottom of Fig. 3 is the total DOS function for $PdTe_2$ calculated by the authors of Ref. 9. A tungsten tip was used to acquire the spectrum in curve D, and PtIr tips were used for the other spectra. Set point currents between 0.03 nA and 0.37 nA were chosen to vary the tunneling gap while containing the amplitude of the ac tunneling current under 40 nA. The need to make provision for the collection of high current values meant a concomitant loss of resolution when measuring very low currents around $V=0$. The use of a sinusoidal voltage oscillation also meant a slightly lower-energy resolution in this part of each I-V curve. Despite being divided by I/V, most spectra in Fig. 3 still tend to rise as the voltage moves away from zero. The strong voltage dependence of the tunneling current and the nonzero value of di/dV at $V=0$ are in keeping with $PdTe_2$ being a metal.

There are four features to consider in the experimental STS spectra in Fig. 3. For energy levels above E_F a resonance $U1$ around 0.5 eV is seen in all spectra. In the widest spectra a second peak $U2$ appears around 1.6 eV. A resonance $O1$ at -0.8 eV and a broader one $O2$ occurring between -1.5 eV and -1.6 eV are labeled in the occupied region. The distinctiveness of the features observed in STS spectra vary between curves, appearing less pronounced in data taken from steeper I-V curves with higher dc tunneling currents. Nevertheless, the stringent averaging technique applied in forming each averaged I-V curve and the repetition seen in several experiments with both W and PtIr tips gives confidence that the identified features relate to the electronic structure of the samples.

The right-hand curve in Fig. 4 is an angle-resolved normal-incidence inverse photoemission spectroscopy (IPES) isochromat taken from a $PdTe_2$ sample cleaved *in situ* in a vacuum of $<10^{-10}$ Torr. This data was recorded at a photon energy of 11.4 eV using an electron beam with an estimated maximum uncertainty in k parallel of ~ 0.14 Å^{-1}. The details of the bandpass detector used to collect the data have been reported elsewhere.[15] Two important features of interest in the isochromat occur at 0.5 eV and 1.7 eV. These peaks, labeled $J1$ and $J2$, indicate transitions into unoccupied bulk conduction bands of the sample. The energy assignments were made by taking the Fermi level to be at the midpoint of the leading edge of a freshly evaporated Au sample that was in electrical contact with the $PdTe_2$ sample.

The appearance of $J1$ and $J2$ in a normal-incidence spectrum allows them to be identified as transitions into unoccupied bulk conduction bands occurring along the ΓA symmetry line of the Brillouin zone [see Fig. 1(b)]. Further analysis of their k-space locations would require assumptions to be made about their initial states. Nevertheless, the band-structure plot for $PdTe_2$ calculated by Guo and Liang[9] shows Γ point energies occurring at 0.7 eV, and 1.9 eV, and an A point energy at 1.7 eV. The states predicted to exist at the

TABLE I. List of states predicted at Γ and *A* for $PdTe_2$ [Data taken from Guo and Liang (1986) (Ref. 9).] Note that the authors' calculations indicate that the $d(zx,yz)/p(xy)$ band is predominantly tellurium in character.

States at Γ(eV)	Bonding character	States at *A* (eV)	Bonding character	DOS peak positions (eV)
1.9	$p(z)$	1.7	$d(zx,yz)/p(xy)$	1.6
0.7	$d(zx,yz)/p(xy)$			0.5
0.1	$p(xy)$			
		−0.7	$p(xy)$	
		−1.4	$p(z)$	−1.5
		−1.6	$d(z^2)$	
−2.7	$d(z^2)$			−2.7
−4.1	$d(xy,x^2-y^2)$	−4.1	$d(xy,x^2-y^2)$	−4.1

Γ point and at the *A* point of the Brillouin zone are listed in Table I together with their bonding character. The peak *J*2 in Fig. 4 is broader than *J*1 and may contain contributions from two unresolved transitions with similar final-state energies close to 1.7 eV. The intensity of the IPES spectrum in Fig. 4 drops distinctively after the *J*2 peak indicating a gap between the lower and upper conduction bands of approximately 1 eV. The strong feature at the start of the upper conduction band around 4.8 eV is believed to be an image state, and further confirmatory work is in progress.

The left-hand side of Fig. 4 shows a normal-emission photoemission spectroscopy (PES) spectrum taken off a $PdTe_2$ sample by Orders and co-workers[6,16] using a Ne I (16.8 eV) photon beam. Peaks in this PES spectrum correspond to transitions occurring along the Γ*A* symmetry line from bulk bands, with a more specific *k*-space determination requiring assumptions to be made about the final-state bands. From Table I it can, however, be seen that the occupied states predicted at *A* and at Γ are consistent with many of the peaks in the PES spectrum.

It is usual, following the theoretical analysis of Tersoff and Hamann,[17] to compare STS spectra with a calculation of the sample's DOS. Good agreement can be seen between the features, *O*1, *O*2, *U*1, and *U*2, in Fig. 3 and peaks and shoulders in the theoretical DOS function reproduced from Ref. 9 at the foot of the figure. The availability of angle-resolved PES and IPES spectra (where only the normal results have been displayed in Fig. 4) allows the extent to which the STS data is *k* resolved to be considered. For unoccupied energy levels, it can be seen that the peaks *J*1 and *J*2 in Fig. 4 match the resonances *U*1 and *U*2 in Fig. 3. From the voltage ramps taken to 2 V in Fig. 3, it is clear that the state at *U*2 is more prominent than the state at *U*1. This result indicates the STS technique is more sensitive to states existing at the *A* point than it is to those occurring at the Γ point, as discussed in Ref. 13. The appearance of *O*1 and *O*2 in the STS spectra for energies below the Fermi level further illustrates the sensitivity of STS to states existing at the *A* point.

From Table I it can be seen that the source of the electrons responsible for the features labeled *O*1, *U*1, and *U*2 in Fig. 3 are the *p* bands of the tellurium atoms. The two predicted states at −1.4 eV and −1.6 eV appear as a single peak in both the STS and PES spectra. It is not possible to determine the principal source of this feature as one of the predicted states has a metal *d* character and the other has a chalcogen *p* character. The STS peaks *O*1 and *O*2 occur marginally closer to E_F in the STS spectra than in the PES spectra, a result which is consistent with the relevant bands in the LAH plane [see Fig. 1(b)] having minima at the *A* point.[6,9] The inclusion of some off-normal electrons in the STS peaks would push them to energies marginally higher than the normal-emission peaks.

Once features in a sample's STS spectra are linked to peaks in its PES and IPES spectra, knowledge of the material's band structure can be used to interpret the STM images. The photoemission results and subsequent theoretical calculations indicate that there is heavy mixing of the chalcogen *p* bands and metal *d* bands in $PdTe_2$,[6,9,16] so that both tellurium and palladium electrons are possible sources of the high intensity spots in Fig. 2. The STS experiments on $PdTe_2$ were performed after STM imaging no longer produced atomic resolution images. It can therefore be presumed that the tunneling current signals giving rise to the STS results in Fig. 3 have averaged the DOS of the sample over a number of atomic sites with tellurium and palladium states feeding into the tunneling current. This mixing may be reflected in the position of some of the STS peaks, with, for example, the broad *O*2 peak seen around −1.6 eV likely to include contributions from both the $p(z)$ and $d(z^2)$ electron states. The appearance of regions of intermediate intensity along the $[10\bar{1}0]$ direction in some parts of the images in Fig. 2 is also consistent with both tellurium *p* states and palladium *d* states contributing to the tunneling current signal.

The one clear point to emerge from the STM images in Fig. 2 is that electrons from one species of atom, either palladium or tellurium, are the stronger contributors to the tunneling current at low bias voltages. The STS results together with the accepted geometric order of the tellurium and palladium layers allow this indetermination to be resolved. Apart from a state at 0.1 eV, which is not sufficiently resolved, the states within 2 eV of the Fermi level that are expected to have a chalcogen *p* character are seen in Fig. 3. The STS spectra clearly indicate that tellurium atoms are contributing electrons to the tunneling current at low bias voltages on both sides of the Fermi energy. While it is unlikely that these atoms are the exclusive source of the tunneling current from $PdTe_2$ samples, the fact that these atoms are expected to occupy the uppermost positions in the crystal lattice makes them the most likely source of the strongest signal. It is thus considered that the positions where the tunneling current has the highest intensity in the images in Fig. 2 are the positions of tellurium atoms in the topmost layer of the material.

In conclusion, IPES and STS have been used to identify two unoccupied bulk states at 0.5 eV and 1.7 eV in the metallic layered compound $PdTe_2$. A number of previously identified occupied bulk states also occur in the STS spectra. The position of the resonances in the STS spectra fit closely with the position of the peaks seen in the normal-incidence IPES and normal-emission PES spectra. Identifying features in the STS spectra of $PdTe_2$ with states known to exist at the *A* point and at the Γ point of the Brillouin zone provides experimental evidence that electron wave functions extend-

ing out from the sample surface are strong contributors to the tunneling current for this sample.[18] From a knowledge of the band structure of $PdTe_2$, it is possible to conclude that tellurium *p* electrons are the principal source of the tunneling current in $PdTe_2$ images obtained at low bias voltages.

The authors wish to thank L. D. Broekman and S. Tkatchenko for their assistance with the STS measurements taken in UHV, J. Tornallyay, R. Polglase, R. Slee, H. Dressel, W. Trapp, and M. Maclean for their technical assistance, and P. J. Orders and A. P. Stampfl for their helpful discussions.

[1] See, for example, B. Reihl, J. K. Gimzewski, J. M. Nicholls, and E. Tosatti, Phys. Rev. B **33**, 5770 (1986); W. J. Kaiser and R. C. Jaklevic, IBM J. Res. Dev. **30**, 411 (1986); C. K. Shih, R. M. Feenstra, J. R. Kirtley, and G. V. Chandrashekhar, Phys. Rev. B **40**, 2682 (1989); Ju-Jin Kim, I. Ekvall, and H. Olin, *ibid.* **54**, 2244 (1996).

[2] G. Binnig, K. H. Frank, H. Fuchs, N. Garcia, B. Reihl, H. Rohrer, F. Salvan, and A. R. Williams, Phys. Rev. Lett. **55**, 991 (1985).

[3] R. J. Hamers, R. M. Tromp, and J. E. Demuth, Phys. Rev. Lett. **56**, 1972 (1986).

[4] R. M. Feenstra, J. A. Stroscio, J. Tersoff, and A. P. Fein, Phys. Rev. Lett. **58**, 1192 (1987).

[5] See, for example, L. C. Davis, M. P. Everson, R. C. Jaklevic, and W. Shen, Phys. Rev. B **43**, 3821 (1991).

[6] P. J. Orders, J. Liesegang, R. C. G. Leckey, J. G. Jenkin, and J. D. Riley, J. Phys. F **12**, 2737 (1982).

[7] S. L. Tang, R. V. Kasowski, A. Suna, and B. A. Parkinson, Surf. Sci. **238**, 280 (1990); B. A. Parkinson, J. Ren, and M-H. Whangbo, J. Am. Chem. Soc. **113**, 7833 (1991); A. Crossley, S. Myhra, and C. J. Sofield, Surf. Sci. **318**, 39 (1994); S. W. Hla, V. Marinkovic, A. Prodan, and I. Musevic, *ibid.* **352-354**, 105 (1996); A. Saidi, A. Hasbach, W. Raberg, and K. Wandelt, J. Vac. Sci. Technol. A **16**, 951 (1998).

[8] See J. A. Wilson and A. D. Yoffe, Adv. Phys. **18**, 193 (1969); A. A. Balchin, in *Crystallography and Crystal Chemistry of Materials with Layered Structures*, edited by F. Levy (Reidel, Dordrecht, 1976), pp. 1–50. $PdTe_2$ has useful lubricating properties and becomes superconducting below 1.8 K.

[9] G. Y. Guo and W. Y. Liang, J. Phys. C **19**, 5365 (1986), using the linear muffin-tin orbital with atomic sphere approximation method.

[10] M. Weimer, J. Kramar, C. Bai, and J. D. Baldeschwieler, Phys. Rev. B **37**, 4292 (1987); D. C. Dahn, M. O. Watanabe, B. L. Blackford, and M. H. Jericho, J. Appl. Phys. **63**, 315 (1988).

[11] S. Furuseth, S. Kari, and A. Kjekshus, Acta Chem. Scand. **19**, 257 (1965).

[12] See, for example, R. M. Feenstra, W. A. Thompson, and A. P. Fein, Phys. Rev. Lett. **56**, 608 (1986); P. J. M. van Bentum, H. van Kempen, L. E. C. van de Leemput, and P. A. A. Teunissen, *ibid.* **60**, 369 (1988).

[13] R. M. Feenstra, J. A. Stroscio, and A. P. Fein, Surf. Sci. **181**, 295 (1987).

[14] G. W. Ryan and J. Tornallyay, J. Appl. Phys. **85**, 6290 (1999).

[15] W. Sheils, R. C. G. Leckey, and J. D. Riley, Rev. Sci. Instrum. **64**, 1194 (1993).

[16] P. J. Orders, Ph.D. thesis, La Trobe University, Australia, 1980.

[17] J. Tersoff and D. R. Hamann, Phys. Rev. B **31**, 805 (1985).

[18] Compare the theoretical discussion in N. D. Lang, Phys. Rev. Lett. **55**, 230 (1985); C. J. Chen, J. Vac. Sci. Technol. A **9**, 44 (1991).